

## Influence of the Phenyl Side Chain on the Conformation of Cyclopropane Analogues of Phenylalanine

Carlos Alemán,<sup>\*,†</sup> Ana I. Jiménez,<sup>‡</sup> Carlos Cativiela,<sup>‡</sup> Juan J. Perez,<sup>†</sup> and Jordi Casanovas<sup>\*,§</sup>

Departament d'Enginyeria Química, E.T.S. d'Enginyers Industrials, Universitat Politècnica de Catalunya, Diagonal 647, 08028 Barcelona, Spain, Departamento de Química Orgánica, ICMA, Universidad de Zaragoza-CSIC, 50009 Zaragoza, Spain, and Departament de Química, Escola Universitària Politècnica, Universitat de Lleida, c/Jaume II n° 69, 25001 Lleida, Spain

Received: June 25, 2002; In Final Form: August 19, 2002

Quantum mechanics methods have been applied to investigate the effects of the selective orientation of the side chains on the conformational features of cyclopropane analogues of phenylalanine. For this purpose, the conformational preferences of the *N*-acetyl-*N'*-methylamide derivative of 1-aminocyclopropanecarboxylic acid (Ac<sub>3</sub>c) have been compared to those of two stereoisomers of 1-amino-2-phenylcyclopropanecarboxylic acid: (2*S*,3*S*)c<sub>3</sub>Phe and (2*S*,3*R*)c<sub>3</sub>Phe. Geometry and vibration frequencies were calculated by the HF, B3LYP, or MP2 methods using the 6-31G(d) basis set, whereas the energy was further evaluated using, in some cases, more sophisticated methods and larger basis sets. Solvent effects were modeled by the self-consistent polarization continuum model with the HF/6-311G(d,p) method. The stereochemistry of the phenyl side chain largely influences the specific backbone...side chain interactions, which in turn affect the stability of the different conformations. Furthermore, results have been compared with recently published experimental data.

### Introduction

In the last two decades, there has been a considerable interest in the conformational properties of modified amino acids.<sup>1</sup> Among them,  $\alpha,\alpha$ -dialkylated analogues have probably been the most extensively studied. This is because substitution of the  $\alpha$ -carbon hydrogen by an alkyl group usually induces drastic changes in the conformational properties. Indeed, such modification is frequently associated with the incorporation of strong stereochemical constraints, and therefore,  $\alpha,\alpha$ -disubstituted amino acids are in general described as *conformationally restricted*.

The simplest  $\alpha,\alpha$ -dialkylated amino acid is the  $\alpha$ -amino-isobutyric acid (Aib), also denoted  $\alpha$ -methylalanine, in which a methyl group replaces the  $\alpha$ -carbon hydrogen of alanine (Ala). The strong propensity of Aib-based peptides to adopt helical conformations has been reported in a number of theoretical and experimental studies.<sup>2,3</sup> This secondary structure is stabilized by the van der Waals interactions provided by the additional methyl group. Comparison between the potential energy surfaces  $E = E(\varphi, \psi)$  of Aib and Ala indicates that the incorporation of the second methyl group reduces the flexibility of the backbone, with the conformational freedom of the former amino acid being more restricted than that of the latter.<sup>4</sup>

The cyclic homologue of Aib, 1-aminocyclopropanecarboxylic acid (Ac<sub>3</sub>c), is among the  $\alpha,\alpha$ -dialkylated amino acids with stronger stereochemical constraints. These are induced by the highly strained cyclopropane ring, which restricts the flexibility of the backbone. The strong influence of the bond between the two  $\beta$ -carbon atoms in the conformational freedom of the

backbone was recently examined by comparing the potential energy surfaces of the Aib and Ac<sub>3</sub>c model dipeptides.<sup>4a</sup>

Among the strategies employed to design peptides and peptidomimetics with controlled fold in the backbone is the incorporation of selectively oriented side substituents to the conformationally restricted amino acids.<sup>5</sup> Thus, side substituents may help to modulate the conformations of such amino acids by introducing specific interactions with the backbone able to smooth the existing stereochemical constraints or even to add new ones. In this context, the substituted derivatives of Ac<sub>3</sub>c deserve special attention because, in addition to the restrictions imposed by  $\alpha,\alpha$ -dialkylation, the rigidity of the three-membered ring fixes the side chain in a well-defined orientation, and this disposition is different for each stereoisomer. The cyclopropane analogue of phenylalanine (1-amino-2-phenylcyclopropanecarboxylic acid, c<sub>3</sub>Phe) is particularly attractive because the rigidly oriented phenyl side chain may interact with the backbone not only sterically but also electronically through the aromatic  $\pi$  orbitals. As a matter of fact, the latter point has been recognized as an important factor in peptide and protein structure.<sup>6,7</sup> Because of these peculiar structural features, c<sub>3</sub>Phe has been incorporated into aspartame,<sup>8</sup> enkephalin,<sup>9</sup> substance P,<sup>10</sup> and an antiopiate tetrapeptide.<sup>11</sup> Moreover, c<sub>3</sub>Phe-containing peptides have proven to be more resistant to enzymatic degradation than their parent compounds.<sup>9c,11b,12</sup>

Despite its interest, the number of works devoted to study the structure of c<sub>3</sub>Phe is very scarce. The molecular conformation of all four stereoisomers of c<sub>3</sub>Phe within the model tripeptide RCO-L-Pro-c<sub>3</sub>Phe-NHMe has recently been investigated by some of us using X-ray crystallography, NMR, and IR spectroscopy<sup>13</sup> and has been found to be greatly dependent on the c<sub>3</sub>Phe stereochemistry, i.e., on the orientation of the phenyl ring with respect to the peptide backbone. On the other hand, Burgess and co-workers reported a theoretical study on some c<sub>3</sub>Phe stereoisomers.<sup>11,14</sup> Calculations consisted of energy

\* To whom correspondence should be addressed. E-mail: carlos.aleman@upc.es; jcasanovas@quimica.udl.es.

<sup>†</sup> Universitat Politècnica de Catalunya.

<sup>‡</sup> Universidad de Zaragoza-CSIC.

<sup>§</sup> Universitat de Lleida.

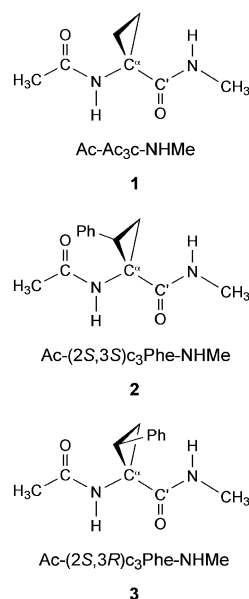


**Figure 1.** Molecular structures of the dipeptides investigated in this work.

minimizations using molecular mechanics, and the force-field parameters were directly transferred from the standard CHARMM force field.<sup>15</sup> This is in contradiction with the results reported by other authors, which stated that standard force fields cannot properly account for the conformational preferences of cyclopropane-based amino acids.<sup>16</sup> Specifically, conventional force fields are not able to reflect either the strained nature of the ring or the hyperconjugative effects observed in cyclopropane derivatives directly associated to a carbonyl group.<sup>17</sup>

In this work, we wish to provide an extensive quantum mechanical study about the conformational preferences of c<sub>3</sub>Phe. First, in order to choose an appropriate computational strategy, the conformational properties of the *N*-acetyl-*N*'-methylamide derivative of Ac<sub>3</sub>c (Ac-Ac<sub>3</sub>c-NHMe, **1**) have been reinvestigated using different quantum mechanical methods. Next, the conformational changes induced by the substitution of a  $\beta$  hydrogen for a phenyl group in the cyclopropane ring of **1** have been analyzed. For this purpose, the analogous dipeptides incorporating (2*S*,3*S*)c<sub>3</sub>Phe (**2**) and (2*S*,3*R*)c<sub>3</sub>Phe (**3**) have been examined. The molecular structures of all of the compounds investigated are displayed in Figure 1. It should be noted that the two c<sub>3</sub>Phe stereoisomers selected for the present study are analogues of L-phenylalanine (*S* configuration at the  $\alpha$  or 2 carbon), whereas their respective enantiomers, (2*R*,3*R*)c<sub>3</sub>Phe and (2*R*,3*S*)c<sub>3</sub>Phe, are D-phenylalanine derivatives.

### Computational Details

Calculations were performed on the IBM/SP2 and HP-V2500 computers of the "Centre de Supercomputació de Catalunya" using the Gaussian 98 and Gaussian 94 programs.<sup>18</sup> Molecular geometries of all of the conformations considered for **1** were optimized in the gas phase at the HF/6-31G(d),<sup>19</sup> B3LYP/6-31G(d),<sup>20</sup> and MP2/6-31G(d)<sup>21</sup> levels of theory, whereas conformations for **2** and **3** were optimized at the HF/6-31G(d) and B3LYP/6-31G(d) levels. The default force and displacement termination criteria within Gaussian 98 were used for all optimizations. All of the stationary points located were characterized as minima by harmonic vibrational frequency calculations. Frequency analysis was also used to provide the zero-point vibrational energy (ZPE), the thermal correction to the energy, and the entropy following the standard for-

**TABLE 1: Torsional Angles (in Degrees) and Enthalpy Differences in the Gas Phase (in kcal/mol) for the Minimum Energy Conformations of Ac-Ac<sub>3</sub>c-NHMe (**1**) Obtained at the HF/6-31G(d), B3LYP/6-31G(d), and MP2/6-31G(d) Levels**

#	$\omega_1$	$\varphi$	$\psi$	$\omega_2$	$\Delta H_{\text{gp}}$
HF/6-31G(d) <sup>a</sup>					
C <sub>7</sub>	-174.3	-78.9	31.7	172.9	0.0 <sup>b</sup>
C <sub>5</sub>	-179.9	180.0	179.9	180.0	3.2
P <sub>II</sub>	165.4	71.2	-145.6	-176.9	2.6
B3LYP/6-31G(d)					
C <sub>7</sub>	-176.4	-73.7	37.4	174.3	0.0 <sup>c</sup>
C <sub>5</sub>	180.0	180.0	180.0	180.0	2.3
MP2/6-31G(d)					
C <sub>7</sub>	-173.6	-77.3	34.1	-172.4	0.0 <sup>d</sup>
C <sub>5</sub>	180.0	180.0	179.9	180.0	2.5

<sup>a</sup> From ref 4a. <sup>b</sup>  $E = -530.475625$  au. <sup>c</sup>  $E = -533.565777$  au. <sup>d</sup>  $E = -532.061863$  au.

mulas. Single-point energy calculations were performed at the B3LYP/6-31G(d), MP2/6-31G(d), B3LYP/6-311G(d,p), MP2/6-311G(d,p), and MP4/6-31G(d) levels.

The effect of the solvent in the conformational preferences of the compounds under study was estimated using the polarizable continuum model (PCM) developed by Tomasi and co-workers.<sup>22</sup> The PCM model represents the polarization of the liquid by a charge density appearing on the surface of the cavity created in the solvent. This cavity is built using a molecular shape algorithm. PCM calculations were performed in the framework of the ab initio HF level because electron correlation effects are not required to obtain reliable values of the free energy of solvation.<sup>22b</sup> Calculations were carried out with a 6-311G(d,p) basis set and using the standard protocol. Because the change of the molecular geometry upon solvation has a negligible effect on the thermodynamic parameters, only gas phase optimized geometries were used.<sup>23</sup> The following dielectric constants were considered in the calculations:  $\epsilon = 2$  for CCl<sub>4</sub>,  $\epsilon = 4$  for CHCl<sub>3</sub>,  $\epsilon = 8$  for CH<sub>2</sub>Cl<sub>2</sub>,  $\epsilon = 33$  for CH<sub>3</sub>OH, and  $\epsilon = 78.5$  for H<sub>2</sub>O.

### Results and Discussion

**Ac-Ac<sub>3</sub>c-NHMe (**1**).** Our previous results<sup>4a</sup> derived from HF/6-31G(d) geometry optimizations on **1** have been summarized in Table 1. A systematic exploration of the conformational space allowed us to characterize three minimum energy conformations at this level of theory. The global minimum was the C<sub>7</sub> (seven-membered hydrogen bonded ring) or  $\gamma$ -turn conformation with dihedral angles  $\varphi, \psi = -78.9^\circ, 31.7^\circ$ . The fully extended conformation, also denoted C<sub>5</sub> (five-membered hydrogen bonded ring), was 3.2 kcal/mol higher in energy than the global minimum. The hydrogen bonding parameters characterized for the C<sub>7</sub> and C<sub>5</sub> conformations were  $d(\text{H}\cdots\text{O}) = 2.162$  Å,  $\angle\text{N}-\text{H}\cdots\text{O} = 146.2^\circ$  and  $d(\text{H}\cdots\text{O}) = 2.065$  Å,  $\angle\text{N}-\text{H}\cdots\text{O} = 110.4^\circ$ , respectively. Finally, the P<sub>II</sub> (polyproline II) conformation was 2.6 kcal/mol unfavored with respect to the global minimum. This conformation is not stabilized by any intramolecular hydrogen bond but minimizes the steric repulsion between the amide groups and the  $\beta$ -methylene hydrogen atoms observed in the C<sub>5</sub> arrangement.<sup>4a</sup> It should be noted that both the C<sub>7</sub> and P<sub>II</sub> minima are 2-fold degenerated because of the achiral nature of the compound, i.e.  $\varphi, \psi = -\varphi, -\psi$ .

The three HF/6-31G(d) structures were used as starting points for complete geometry optimization at the B3LYP/6-31G(d) and MP2/6-31G(d) levels. Only two minima, which correspond to the C<sub>7</sub> and C<sub>5</sub> conformations, were characterized at these levels

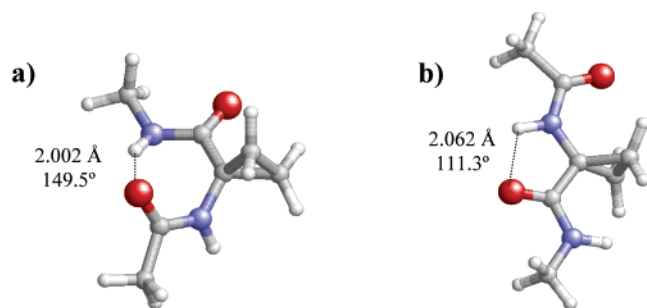


**Figure 2.**  $C_7$  (a) and  $C_5$  (b) minimum energy conformations of Ac-Ac<sub>3</sub>c-NHMe (**1**) obtained at the MP2/6-31G(d) level of theory. Hydrogen bonding distances (H...O) and angles (N–H...O) are indicated.

of theory, with their dihedral angles being displayed in Table 1. The inclusion of electron correlation effects implied the loss of the  $P_{II}$  conformation as a potential energy minimum. We illustrate the  $C_7$  and  $C_5$  minima characterized at the MP2/6-31G(d) level in Figure 2. The B3LYP and MP2 geometrical parameters are very similar (see the Supporting Information), the maximum deviations being 0.014 Å, 0.4° and 3.6° for bond lengths, bond angles and dihedral angles, respectively. From this comparison, we conclude that it is sufficient to carry out the geometry optimizations with the B3LYP method, and therefore, it may be unnecessary to perform them at the MP2 level. This is useful information as such optimizations on the compounds with phenyl side chain can be very time-consuming.

A detailed inspection to Table 1 reveals an interesting geometric trend. This concerns the value of the dihedral angle  $\psi$  for the  $C_7$  conformation ( $\psi = 34.1^\circ$  at the MP2 level), which is considerably smaller than that predicted for the  $C_7$  conformation of analogous dipeptides constituted by standard amino acids, like Gly ( $\psi = 75.5^\circ$ ),<sup>24a</sup> Ala ( $\psi = 79.1^\circ$ ),<sup>4b,24a</sup> Asn ( $\psi = 62.6^\circ$ ),<sup>24b</sup> or Asp ( $\psi = 71.4^\circ$ ).<sup>24c</sup> This tendency to adopt a small value of  $\psi$  is explained by the hyperconjugation between the lone pairs of the carbonyl oxygen belonging to the Ac<sub>3</sub>c residue and the adjacent  $\sigma^* C^\beta-C^{\beta'}$  molecular orbitals.<sup>17a</sup> Thus, the C=O bond tends to be arranged in such a way that it bisects the  $\angle C^\beta-C^\alpha-C^{\beta'}$  angle, and this disposition corresponds to  $\psi$  values near  $0^\circ$ . Furthermore, X-ray diffraction analysis of Ac<sub>3</sub>c-containing peptides evidence that this conformationally restricted amino acid tends to adopt dihedral values  $\varphi, \psi$  about  $\pm 80^\circ, 0^\circ$  (the so-called *bridge* region)<sup>25</sup> and thus to be accommodated in the  $i+2$  position of types I and II  $\beta$ -turns. It should be emphasized that dipeptide **1** is not long enough to form a  $\beta$ -turn (a minimum of two residues is required to allow intramolecular hydrogen bonding), and as a consequence, the stability of conformations in the neighborhood of  $\varphi, \psi = \pm 80^\circ, 0^\circ$  can be underestimated in favor of  $C_7$ -like structures. Moreover, these  $\varphi, \psi$  values can be attained through a distortion of only 30–35° in the  $\psi$  angle of the  $C_7$  minimum characterized for **1**.

With regard to the geometry of the Ac<sub>3</sub>c residue, results show a dependence of the  $\angle N-C^\alpha-C'$  bond angle on the conformation. More specifically, this conformationally informative parameter varies from 119° ( $C_7$ ) to 108° ( $C_5$ ). The value of the  $\angle N-C^\alpha-C'$  angle in the  $C_7$  conformation is considerably larger than the expected tetrahedral value. A similar conformational dependence for such a bond angle was also detected in other constrained amino acids such as for instance dehydroalanine ( $\Delta$ Ala).<sup>26</sup>

The effects of the level of geometry optimization, the basis set expansion and the electron correlation on the enthalpy differences in the gas phase ( $\Delta H_{gp}$ ) are displayed in Table 2.

**TABLE 2: Enthalpy Differences in the Gas Phase (in kcal/mol) for the Minimum Energy Conformations Characterized for Ac-Ac<sub>3</sub>c-NHMe (**1**)**

level <sup>a</sup>	$C_7$	$C_5$	$P_{II}$
HF/6-31G(d)//HF/6-31G(d) <sup>b,c</sup>	0.0 <sup>d</sup>	3.2	2.6
B3LYP/6-31G(d)//HF/6-31G(d) <sup>c</sup>	0.0 <sup>e</sup>	1.8	4.0
MP2/6-31G(d)//HF/6-31G(d) <sup>c</sup>	0.0 <sup>f</sup>	3.0	3.8
B3LYP/6-311G(d,p)//HF/6-31G(d) <sup>c</sup>	0.0 <sup>g</sup>	1.7	3.6
MP2/6-311G(d,p)//HF/6-31G(d) <sup>c</sup>	0.0 <sup>h</sup>	2.8	3.1
B3LYP/6-31G(d)//B3LYP/6-31G(d) <sup>i</sup>	0.0 <sup>j</sup>	2.3	-
MP2/6-31G(d)//B3LYP/6-31G(d) <sup>i</sup>	0.0 <sup>k</sup>	3.5	-
B3LYP/6-311G(d,p)//B3LYP/6-31G(d) <sup>i</sup>	0.0 <sup>l</sup>	2.2	-
MP2/6-311G(d,p)//B3LYP/6-31G(d) <sup>i</sup>	0.0 <sup>m</sup>	3.1	-
MP2/6-31G(d)//MP2/6-31G(d) <sup>n</sup>	0.0 <sup>o</sup>	2.5	-
B3LYP/6-31G(d)//MP2/6-31G(d) <sup>n</sup>	0.0 <sup>p</sup>	1.4	-
B3LYP/6-311G(d,p)//MP2/6-31G(d) <sup>n</sup>	0.0 <sup>q</sup>	1.1	-
MP2/6-311G(d,p)//MP2/6-31G(d) <sup>n</sup>	0.0 <sup>r</sup>	2.3	-
MP4/6-31G(d)//MP2/6-31G(d) <sup>n</sup>	0.0 <sup>s</sup>	2.4	-
MP2/6-311G(d,p) + MP4#//MP2/6-31G(d) <sup>n</sup>	0.0 <sup>t</sup>	2.3	-

<sup>a</sup> Level of energy calculation // level of geometry optimization.

<sup>b</sup> From ref 4a. <sup>c</sup> Zero-point energies and thermal corrections computed at the HF/6-31G(d) level are included. <sup>d</sup>  $E = -530.475625$  au. <sup>e</sup>  $E = -533.700022$  au. <sup>f</sup>  $E = -532.045888$  au. <sup>g</sup>  $E = -533.853509$  au.

<sup>h</sup>  $E = -532.350128$  au. <sup>i</sup> Zero-point energies and thermal corrections computed at the B3LYP/6-31G(d) level. <sup>j</sup>  $E = -533.565777$  au.

<sup>k</sup>  $E = -532.064543$  au. <sup>l</sup>  $E = -533.870700$  au. <sup>m</sup>  $E = -532.367151$  au. <sup>n</sup> Zero-point energies and thermal corrections computed at the MP2/6-31G(d) level are included. <sup>o</sup>  $E = -532.061863$  au. <sup>p</sup>  $E = -533.714524$  au. <sup>q</sup>  $E = -533.866094$  au. <sup>r</sup>  $E = -532.363962$  au. <sup>s</sup>  $E = -532.194785$  au. <sup>t</sup>  $E = -532.496884$  au.

In all cases, the  $C_7$  conformation was found to be more stable than the  $C_5$  arrangement. However, results show a notable dependence of  $\Delta H_{gp}$  on the computational method used to optimize the molecular geometries. Thus, for a given level of energy calculation, the smallest value was always provided by the MP2/6-31G(d) geometry, whereas the values obtained using the HF/6-31G(d) and B3LYP/6-31G(d) geometries were systematically overestimated by about 0.5 and 1 kcal/mol, respectively. On the other hand, a comparison of the energies provided by the 6-31G(d) and 6-311G(d,p) basis set indicates that  $\Delta H_{gp}$  is quite independent of the basis set expansion. Thus,  $\Delta H_{gp}$  decreases by only about 0.2 kcal/mol when the basis set is enlarged. The best estimate to  $\Delta H_{gp}$  was that obtained with the MP2 correction computed from the 6-311G(d,p) basis set and the small correction up to MP4(SDTQ) calculated at the 6-31G(d) level and added to the MP2/6-311G(d,p), this theoretical level being denoted MP2/6-311G(d,p)+MP4#:

$$H(\text{MP2/6-311G(d,p)+MP4\#}) = H(\text{MP2/6-311G(d,p)}) + [H(\text{MP4/6-31G(d)}) - H(\text{MP2/6-31G(d)})]$$

Accordingly, correlation effects up to fourth order were introduced assuming that the transferability of the correction between MP4 and MP2 levels determined the 6-31G(d) basis set to the MP2/6-311G(d,p) results. The MP2/6-311G(d,p)+MP4# level predicts an enthalpy difference of 2.3 kcal/mol between the  $C_7$  and  $C_5$  conformations when the molecular geometries optimized at the MP2/6-31G(d) level are used.

Table 3 shows the entropic contribution in the gas phase,  $-T\Delta S_{gp}$ , at 298 K for the  $C_7$  and  $C_5$  conformations of **1**. This term is 2.0 kcal/mol larger at the MP2/6-31G(d) level than at the B3LYP/6-31G(d) one, with the latter being 0.9 kcal/mol smaller than that predicted at the HF/6-31G(d) level. The free energy differences between the  $C_7$  and  $C_5$  conformations in the gas phase,  $\Delta G_{gp}$ , predicted by some selected methods have been included in Table 3. Our best estimate to  $\Delta G_{gp}$ , which was 4.5 kcal/mol, reveals that the stability of the  $C_7$  conformation is



**TABLE 3: Free Energy Difference<sup>a</sup>(in kcal/mol) at 298 K in the Gas Phase between the C<sub>7</sub> and C<sub>5</sub> Conformations of Ac-Ac<sub>3</sub>c-NHMe (1) for a Selected Set of Computational Levels<sup>b</sup>**

level <sup>c</sup>	$\Delta H_{\text{gp}}$	$-T\Delta S_{\text{gp}}$	$\Delta G_{\text{gp}}$
HF/6-31G(d)//HF/6-31G(d)	3.2	1.1	4.3
MP2/6-311G(d,p)//HF/6-31G(d)	2.8	1.1 <sup>d</sup>	3.9
B3LYP/6-31G(d)//B3LYP/6-31G(d)	2.3	0.2	2.5
MP2/6-31G(d)//B3LYP/6-31G(d)	3.5	0.2 <sup>e</sup>	3.7
MP2/6-311G(d)//B3LYP/6-31G(d)	3.1	0.2 <sup>e</sup>	3.3
MP2/6-31G(d)//MP2/6-31G(d)	2.5	2.2	4.7
MP2/6-311G(d,p)+MP4#//MP2/6-31G(d)	2.3	2.2 <sup>f</sup>	4.5

<sup>a</sup> Free energy differences at 298 K in the gas phase:  $\Delta G_{\text{gp}} = \Delta H_{\text{gp}} - T\Delta S_{\text{gp}}$ . <sup>b</sup> The enthalpy difference and the entropic correction in the gas phase are also displayed (in kcal/mol). All of the values are relative to the C<sub>7</sub> conformation. <sup>c</sup> Level of energy calculation // level of geometry optimization. <sup>d</sup> Entropic correction calculated at the HF/6-31G(d)//HF/6-31G(d) level. <sup>e</sup> Entropic correction calculated at the B3LYP/6-31G(d)//B3LYP/6-31G(d) level. <sup>f</sup> Entropic correction calculated at the MP2/6-31G(d) level.

**TABLE 4: Free Energy Differences in Solution between the C<sub>7</sub> and C<sub>5</sub> Conformations of Ac-Ac<sub>3</sub>c-NHMe (1)<sup>a</sup>**

	$\epsilon = 2$	$\epsilon = 4$	$\epsilon = 8$	$\epsilon = 33$	$\epsilon = 78.5$
$\Delta G_{\text{sol}}(\text{C}_7)$	-5.5	-9.4	-11.7	-13.8	-14.2
$\Delta G_{\text{sol}}(\text{C}_5)$	-4.9	-8.3	-10.3	-12.1	-12.5
$\Delta G_{\epsilon}^b$	5.1	5.6	5.9	6.2	6.2

<sup>a</sup> Free energies of solvation (in kcal/mol) in the different solvents are also displayed. Differences are relative to the C<sub>7</sub> conformation. Free energies of solvation ( $\Delta G_{\text{sol}}$ ) were computed using the PCM model at the HF/6-311G(d,p) level and considering the molecular geometries optimized in the gas phase at the MP2/6-31G(d) level. <sup>b</sup> Free energy difference in solution at 298 K:  $\Delta G_{\epsilon} = \Delta G_{\text{gp}} + \Delta \Delta G_{\text{sol}}$ . The best estimate of  $\Delta G_{\text{gp}}$  was considered (see Table 3).

considerably influenced by the entropic term. On the other hand, very reasonable estimates to  $\Delta G_{\text{gp}}$  can be obtained using less sophisticated theoretical methods than the MP2/6-311G-(d,p)+MP4#//MP2/6-31G(d) one. For instance, the values derived from HF/6-31G(d)//HF/6-31G(d) and MP2/6-31G(d)//B3LYP/6-31G(d) calculations are 4.3 and 3.7 kcal/mol, respectively. This is an important result because the large size of the c<sub>3</sub>Phe residue precludes the use of sophisticated theoretical methods for dipeptides **2** and **3**.

The free energies of solvation,  $\Delta G_{\text{sol}}$ , derived from PCM calculations at the HF/6-311G(d,p) level are listed in Table 4. As expected, the  $\Delta G_{\text{sol}}$  values decrease when the polarity of the environment increases. The C<sub>7</sub> conformation provides better interactions with the solvent than the C<sub>5</sub> arrangement for the five environments considered. Thus, the relative stability of the latter conformation decreases in solution. Table 4 also shows the free energy differences in solution,  $\Delta G_{\epsilon}$ , which were estimated with a classical thermodynamical scheme by adding the  $\Delta \Delta G_{\text{sol}}$  values to the  $\Delta G_{\text{gp}}$  obtained at the MP2/6-311G-(d,p)+MP4#//MP2/6-31G(d) level. It can be seen that the free energy difference between the two conformations increases from 4.5 kcal/mol in the gas phase (Table 3) to 6.2 kcal/mol in aqueous solution (Table 4).

Figure 3a shows the variation of the dipole moment with the dielectric constant of the environment for the C<sub>7</sub> and C<sub>5</sub> conformations of **1**. It is worth noting that for  $\epsilon \leq 8$  the solvent-induced polarization effects sharply increase with the dielectric constant. Thus, the dipole moments increase by about 11% and 25% on going from the gas phase to solvents with  $\epsilon = 2$  and 8, respectively. Conversely, for  $\epsilon > 8$ , the variation of the dipole moment is smoothed. Thus, solvents with  $\epsilon = 33$  and 78.5

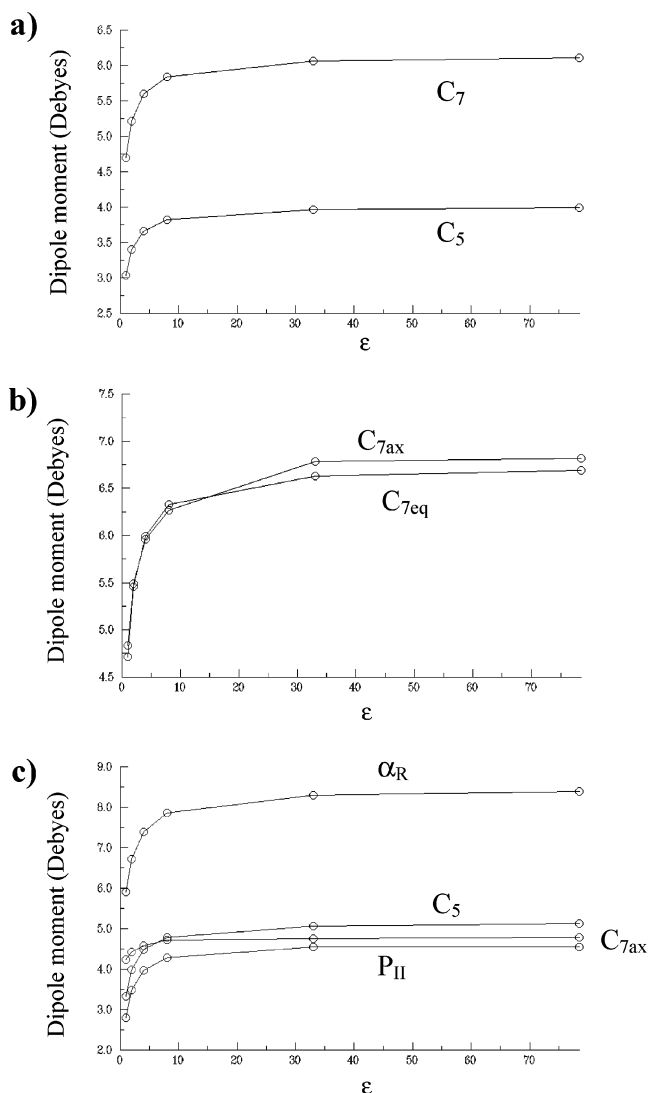


**Figure 3.** Variation of the dipole moment with the dielectric constant of the environment: (a) C<sub>7</sub> and C<sub>5</sub> conformations of Ac-Ac<sub>3</sub>c-NHMe (**1**); (b) C<sub>7eq</sub> and C<sub>7ax</sub> conformations of Ac-(2S,3S)c<sub>3</sub>Phe-NHMe (**2**); and (c) C<sub>7ax</sub>, P<sub>II</sub>, C<sub>5</sub>, and α<sub>R</sub> conformations of Ac-(2S,3R)c<sub>3</sub>Phe-NHMe (**3**).

induce changes in the dipole moments of 29 and 31%, respectively.

**Ac-(2S,3S)c<sub>3</sub>Phe-NHMe (2).** This dipeptide retains the restrictions imposed in **1** by the cyclopropane ring, and additional conformational constraints arise from the presence of the bulky substituent attached to it and situated in a cis relative disposition with respect to the acetamino moiety (Figure 1). Accordingly, the C<sub>7</sub>, C<sub>5</sub>, and P<sub>II</sub> minimum energy conformations characterized for **1** at the HF/6-31G(d) level were considered as good starting geometries for the conformational study of **2**. However, in this case, the C<sub>7</sub> and P<sub>II</sub> conformations are not 2-fold degenerated because of the chiral nature of the molecule, and therefore, the two possibilities,  $\varphi, \psi$  and  $-\varphi, -\psi$ , were taken into account. On the other hand, the dihedral angle  $\chi_1$  is severely restrained by the ring at values near 0°, whereas the flexible dihedral angle  $\chi_2$  is expected to have three different minima (trans, gauche<sup>+</sup>, and gauche<sup>-</sup>). Consequently, a total of  $5 \times 3 = 15$  conformations were initially generated and used as starting points for HF/6-31G(d) geometry optimizations. Three structures were characterized as minimum energy conformations, which were used as starting geometries for subsequent reoptimization at the B3LYP/6-31G(d) level. Only two minima, which

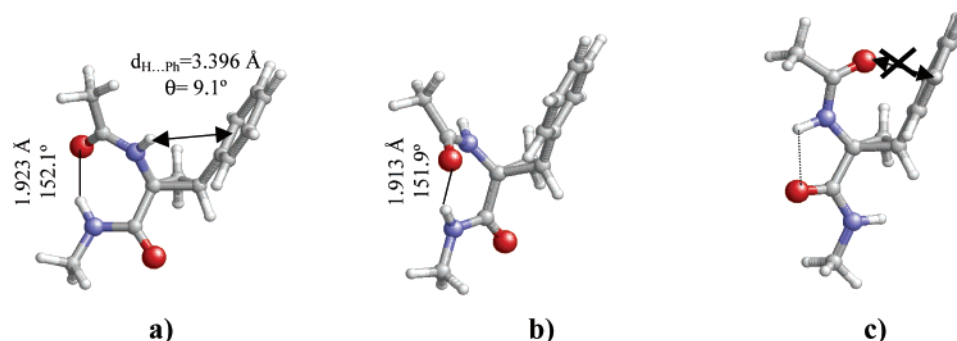


**Figure 4.**  $C_{7eq}$  (a) and  $C_{7ax}$  (b) minimum energy conformations of Ac-(2*S*,3*S*)c<sub>3</sub>Phe-NHMe (**2**) obtained at the B3LYP/6-31G(d) level of theory. (c) Repulsive interaction between the  $\pi$  electron density of the phenyl side chain and the acetyl oxygen for the  $C_5$  conformation (note that it is not a minimum energy conformation). Hydrogen bonding distances (H...O) and angles (N–H...O), as well as the parameters associated to the interaction between the N–H bond and the phenyl ring (H...Ph center distance,  $d_{H...Ph}$ ; N–H...Ph plane angle,  $\theta$ ) are indicated.

**TABLE 5: Torsional Angles (in Degrees) for the Minimum Energy Conformations Characterized for Ac-(2*S*,3*S*)c<sub>3</sub>Phe-NHMe (**2**) and Ac-(2*S*,3*R*)c<sub>3</sub>Phe-NHMe (**3**) at the HF/6-31G(d) and B3LYP/6-31G(d) Levels**

dipep.	#	$\omega_1$	$\varphi$	$\psi$	$\chi_1$	$\chi_2$	$\omega_2$
HF/6-31G(d)							
<b>2</b>	$C_{7eq}$	−171.0	−80.7	31.7	5.7	83.1	173.1
	$C_{7ax}$	169.1	72.3	−21.3	8.4	−104.0	−174.4
	P <sub>II</sub>	−168.4	59.6	−129.2	5.9	−110.4	174.2
<b>3</b>	$C_{7ax}$	−178.9	80.9	−46.7	140.0	−83.6	−173.9
	P <sub>II</sub>	−160.8	76.1	−173.0	140.0	−72.2	178.2
	$C_5$	177.7	−174.0	174.8	136.0	−69.5	175.3
	$\alpha_R$	−171.2	−84.5	−16.0	137.0	108.8	174.9
B3LYP/6-31G(d)							
<b>2</b>	$C_{7eq}$	−173.4	−73.3	35.9	5.6	84.6	174.8
	$C_{7ax}$	170.9	69.1	−28.4	8.0	−106.0	−174.9
<b>3</b>	$C_{7ax}$	177.8	78.0	−46.9	139.0	−86.3	−175.1
	P <sub>II</sub>	−161.7	82.7	−169.0	138.4	−75.1	179.4
	$C_5$	178.0	−176.4	179.6	136.3	−76.6	176.8
	$\alpha_R$	−172.6	−86.1	−16.1	134.3	66.7	176.0

**TABLE 6: Enthalpy Differences in the Gas Phase (in kcal/mol) for the Minimum Energy Conformations of Ac-(2*S*,3*S*)c<sub>3</sub>Phe-NHMe (**2**) and Ac-(2*S*,3*R*)c<sub>3</sub>Phe-NHMe (**3**)**

Ac-(2 <i>S</i> ,3 <i>S</i> )c <sub>3</sub> Phe-NHMe ( <b>2</b> )				
level <sup>a</sup>	$C_{7eq}$	$C_{7ax}$	P <sub>II</sub>	
HF/6-31G(d)//HF/6-31G(d) <sup>b</sup>	0.0 <sup>c</sup>	1.2	4.3	
MP2/6-31G(d)//HF/6-31G(d) <sup>b</sup>	0.0 <sup>d</sup>	0.3	4.7	
B3LYP/6-31G(d)//B3LYP/6-31G(d) <sup>e</sup>	0.0 <sup>f</sup>	0.9	−	
MP2/6-31G(d)//B3LYP/6-31G(d) <sup>e</sup>	0.0 <sup>g</sup>	0.3	−	
Ac-(2 <i>S</i> ,3 <i>R</i> )c <sub>3</sub> Phe-NHMe ( <b>3</b> )				
level <sup>a</sup>	$C_{7ax}$	P <sub>II</sub>	$C_5$	$\alpha_R$
HF/6-31G(d)//HF/6-31G(d) <sup>b</sup>	0.0 <sup>h</sup>	1.4	4.1	3.6
MP2/6-31G(d)//HF/6-31G(d) <sup>b</sup>	0.0 <sup>i</sup>	1.6	3.2	4.7
B3LYP/6-31G(d)//B3LYP/6-31G(d) <sup>e</sup>	0.0 <sup>j</sup>	2.5	2.3	4.2
MP2/6-31G(d)//B3LYP/6-31G(d) <sup>e</sup>	0.0 <sup>k</sup>	1.8	3.1	5.4

<sup>a</sup> Level of energy calculation // level of geometry optimization.

<sup>b</sup> Zero-point energies and thermal corrections computed at the HF/6-31G(d) level are included. <sup>c</sup>  $E = -759.933265$  au. <sup>d</sup>  $E = -762.262646$  au. <sup>e</sup> Zero-point energies and thermal corrections computed at the B3LYP/6-31G(d) level are included. <sup>f</sup>  $E = -764.688049$  au. <sup>g</sup>  $E = -762.288194$  au. <sup>h</sup>  $E = -759.931510$  au. <sup>i</sup>  $E = -762.262055$  au. <sup>j</sup>  $E = -764.686378$  au. <sup>k</sup>  $E = -762.287824$  au.

correspond to the equatorial and axial  $C_7$  conformations ( $C_{7eq}$  and  $C_{7ax}$ , respectively), were characterized at the latter level of theory. Single-point calculations at the MP2/6-31G(d) level were performed for both HF and B3LYP potential energy minima.

Tables 5 and 6 show the dihedral angles and  $\Delta H_{gp}$ , respectively, for the minimum energy conformations of **2**. The inclusion of electron correlation using the B3LYP functional

did not produce significant changes in the molecular geometries of the  $C_{7eq}$  and  $C_{7ax}$  conformations, with the largest change in the dihedral angles being 7.4°. However, B3LYP calculations allowed us to discard the P<sub>II</sub> arrangement as a potential energy minimum, even though it was predicted as such at the HF level.

The lowest energy minimum corresponds to the  $C_{7eq}$  conformation at all of the levels of theory considered, which is also the most favored conformation for the analogous Ala dipeptide.<sup>4b,24a</sup> However, the dihedral angle  $\psi$  is about 45° smaller for **2** than for the Ala dipeptide because of hyperconjugative effects,<sup>17a</sup> as discussed in the previous section for **1**. The  $C_{7eq}$  conformation is a compact structure stabilized by a hydrogen bond with parameters  $d(H...O) = 1.923$  Å and  $\angle N-H...O = 152.1^\circ$  (Figure 4a). Additionally, an N–H... $\pi$  interaction involving the side phenyl ring and one amide group is detected in this conformation. To allow this stabilizing interaction, the phenyl ring adopts a gauche disposition ( $\chi_2 = 83.1^\circ$ ). The parameters used to characterize this interaction are as follows (Figure 4a): (i) the distance between the hydrogen atom of the NH moiety and the center of the ring ( $d_{H...Ph} = 3.396$  Å) and (ii) the angle defined by the N–H bond and the plane of the phenyl ring ( $\theta = 9.1^\circ$ ). Results are consistent with a parallel arrangement between the N–H bond and the phenyl ring. As a matter of fact, the existence of such an attractive interaction between an NH group and the  $\pi$  cloud of the phenyl ring has been invoked to explain the conformational preferences experimentally observed for model peptides incorporating c<sub>3</sub>Phe,<sup>13a</sup> as well as other cyclic phenylalanine analogues.<sup>27</sup>

The  $C_{7ax}$ , which is 0.3 kcal/mol less stable than the  $C_{7eq}$ , is stabilized by an intramolecular hydrogen bond with geometrical parameters  $d(H...O) = 1.913$  Å and  $\angle N-H...O = 151.9^\circ$  (Figure 4b). However, no additional interaction involving the phenyl ring is detected in this case. Thus, the distance  $d_{H...Ph}$  increases to 4.536 Å indicating that the N–H... $\pi$  interaction has not been formed.

Another interesting trend is the annihilation of the  $C_5$  conformation as an energy minimum at both HF and B3LYP levels. This conformation is strongly unfavored for **2** because of the repulsive interaction between the  $\pi$  electron density of the phenyl side chain and the lone pairs of the acetyl carbonyl oxygen (Figure 4c).

Burgess and co-workers reported<sup>11a,14</sup> the conformational preferences of the (2*R*,3*R*)c<sub>3</sub>Phe residue, which is the mirror image of (2*S*,3*S*)c<sub>3</sub>Phe. The authors provided the potential energy surface  $E = E(\varphi, \psi)$ , which was computed using molecular mechanics methods with the standard CHARMM force-field.<sup>15</sup> Two low energy regions were found involving the  $\alpha_R$  (right-handed  $\alpha$ -helical) and  $C_{7ax}$  conformations. On the other

**TABLE 7: Main Structural Parameters<sup>a</sup> for the Minimum Energy Conformations of Ac-(2*S*,3*S*)c<sub>3</sub>Phe-NHMe (2) and Ac-(2*S*,3*R*)c<sub>3</sub>Phe-NHMe (3) Obtained at the B3LYP/6-31G(d) Level**

parameter <sup>b</sup>	Ac-(2 <i>S</i> ,3 <i>S</i> )c <sub>3</sub> Phe-NHMe (2)			Ac-(2 <i>S</i> ,3 <i>R</i> )c <sub>3</sub> Phe-NHMe (3)			
	C <sub>7eq</sub>	C <sub>7ax</sub>	X-ray <sup>c</sup>	C <sub>7ax</sub>	P <sub>II</sub>	C <sub>5</sub>	α <sub>R</sub>
N—C <sup>α</sup>	1.442	1.444	1.436	1.443	1.438	1.439	1.444
C <sup>α</sup> —C <sup>γ</sup>	1.528	1.527	1.503	1.531	1.525	1.523	1.517
C <sup>α</sup> —C <sup>β</sup>	1.526	1.545	1.543	1.536	1.525	1.539	1.552
C <sup>α</sup> —C <sup>β'</sup>	1.523	1.510	1.498	1.505	1.527	1.521	1.509
C <sup>β</sup> —C <sup>β'</sup>	1.499	1.498	1.518	1.502	1.498	1.504	1.499
C <sup>β</sup> —C <sup>γ</sup>	1.497	1.498	1.462	1.497	1.499	1.498	1.496
N—C <sup>α</sup> —C <sup>γ</sup>	119.5	120.3	117.4	117.9	111.6	107.4	117.0
C <sup>β</sup> —C <sup>α</sup> —C <sup>β'</sup>	58.9	58.7	59.9	59.2	58.8	58.9	58.6
C <sup>α</sup> —C <sup>β</sup> —C <sup>β'</sup>	60.4	59.5	58.6	59.4	60.7	59.9	59.3
C <sup>α</sup> —C <sup>β'</sup> —C <sup>β</sup>	60.7	61.8	61.5	61.4	60.5	61.2	62.1

<sup>a</sup> Distances and angles in Å and degrees, respectively. <sup>b</sup> C<sup>β</sup> corresponds to the cyclopropane carbon bearing the phenyl ring; C<sup>γ</sup> is the substituted aromatic carbon. <sup>c</sup> Bond distances and angles for the cyclopropane ring in the crystal molecular structure of Z-L-Pro-(2*S*,3*S*)c<sub>3</sub>Phe-NHMe (ref 13a).

**TABLE 8: Free Energy Differences<sup>a</sup> (in kcal/mol) at 298 K in the Gas Phase among the Minimum Energy Conformations of Ac-(2*S*,3*S*)c<sub>3</sub>Phe-NHMe (2) and Ac-(2*S*,3*R*)c<sub>3</sub>Phe-NHMe (3)<sup>b</sup>**

Ac-(2 <i>S</i> ,3 <i>S</i> )c <sub>3</sub> Phe-NHMe (2)				
level <sup>c</sup>	Δ <i>H</i> <sub>gp</sub>	− <i>T</i> Δ <i>S</i> <sub>gp</sub>	Δ <i>G</i> <sub>gp</sub>	
HF/6-31G(d)//HF/6-31G(d)	1.2	1.2	2.4	
MP2/6-31G(d)//HF/6-31G(d)	0.3	1.2 <sup>d</sup>	1.5	
B3LYP/6-31G(d)//B3LYP/6-31G(d)	0.9	0.8	1.7	
MP2/6-31G(d)//B3LYP/6-31G(d)	0.3	0.8 <sup>e</sup>	1.1	

Ac-(2 <i>S</i> ,3 <i>R</i> )c <sub>3</sub> Phe-NHMe (3)									
level <sup>c</sup>	Δ <i>H</i> <sub>gp</sub>			− <i>T</i> Δ <i>S</i> <sub>gp</sub>			Δ <i>G</i> <sub>gp</sub>		
	P <sub>II</sub>	C <sub>5</sub>	α <sub>R</sub>	P <sub>II</sub>	C <sub>5</sub>	α <sub>R</sub>	P <sub>II</sub>	C <sub>5</sub>	α <sub>R</sub>
HF/6-31G(d)//HF/6-31G(d)	1.4	4.1	3.6	0.6	0.0	−0.9	2.0	4.1	2.7
MP2/6-31G(d)//HF/6-31G(d)	1.6	3.2	4.7	0.6 <sup>d</sup>	0.0 <sup>d</sup>	−0.9 <sup>d</sup>	2.2	3.2	3.8
B3LYP/6-31G(d)//B3LYP/6-31G(d)	2.5	2.3	4.2	0.6	0.7	0.0	3.1	3.0	4.2
MP2/6-31G(d)//B3LYP/6-31G(d)	1.8	3.1	5.4	0.6 <sup>e</sup>	0.7 <sup>e</sup>	0.0 <sup>e</sup>	2.4	3.8	5.4

<sup>a</sup> Free energy differences at 298 K in the gas phase: Δ*G*<sub>gp</sub> = Δ*H*<sub>gp</sub> − *T*Δ*S*<sub>gp</sub>. <sup>b</sup> The enthalpy difference and the entropic correction in the gas phase are also displayed (in kcal/mol). Values are relative to the C<sub>7eq</sub> and C<sub>7ax</sub> conformations for 2 and 3, respectively. <sup>c</sup> Level of energy calculation // level of geometry optimization. <sup>d</sup> Entropic correction calculated at the HF/6-31G(d)//HF/6-31G(d) level. <sup>e</sup> Entropic correction calculated at the B3LYP/6-31G(d)//B3LYP/6-31G(d) level.

hand, the regions around the C<sub>7eq</sub> and α<sub>L</sub> conformations were predicted to be slightly disfavored with respect to the former ones. Comparison with the results provided in the present work indicates that the stability of the helical regions found in such studies is probably due to the simplicity of the computational method. However, the most striking difference between quantum mechanical and force-field results involves the absence of any hyperconjugative effect in the latter. Thus, the dihedral angles ψ associated to the C<sub>7</sub> conformations predicted by molecular mechanics (ψ = −85°/80°)<sup>11a,14</sup> were similar to those provided for nonrestricted amino acids. This deficiency must be attributed to the CHARMM parameters, which were specifically developed to study peptides and proteins constituted by the 20 common amino acids.

Table 7 shows the geometric parameters for the cyclopropane ring in the C<sub>7eq</sub> and C<sub>7ax</sub> conformations of 2. For the sake of completeness, the parameters determined by X-ray diffraction for the only crystalline structure reported<sup>13a</sup> for a (2*S*,3*S*)c<sub>3</sub>Phe-containing peptide have been included. There is a good agreement between the experimental and theoretical values, with the average error in bond lengths and angles being 0.019 Å and 1.3°, respectively. It should be noted that in all cases the bond angle ∠N—C<sup>α</sup>—C<sup>γ</sup> largely exceeds the standard tetrahedral value. On the other hand, the C<sup>β</sup>—C<sup>γ</sup> bond length is slightly shorter than expected for a typical C(sp<sup>3</sup>)—C(sp<sup>2</sup>) bond, a feature that can be ascribed to the conjugative capabilities of the cyclopropane ring.

**TABLE 9: Free Energy Differences in Solution between the Minimum Energy Conformations of Ac-(2*S*,3*S*)c<sub>3</sub>Phe-NHMe (2) and Ac-(2*S*,3*R*)c<sub>3</sub>Phe-NHMe (3)<sup>a</sup>**

	ε = 2	ε = 4	ε = 8	ε = 33	ε = 78.5
Ac-(2 <i>S</i> ,3 <i>S</i> )c <sub>3</sub> Phe-NHMe (2)					
Δ <i>G</i> <sub>sol</sub> (C <sub>7eq</sub> )	−5.7	−9.6	−12.1	−14.2	−14.7
Δ <i>G</i> <sub>sol</sub> (C <sub>7ax</sub> )	−5.2	−8.7	−10.9	−12.8	−13.2
Δ <i>G</i> <sub>ε</sub> <sup>b</sup>	1.6	2.0	2.3	2.5	2.6
Ac-(2 <i>S</i> ,3 <i>R</i> )c <sub>3</sub> Phe-NHMe (3)					
Δ <i>G</i> <sub>sol</sub> (C <sub>7ax</sub> )	−5.1	−8.6	−10.7	−12.5	−12.9
Δ <i>G</i> <sub>sol</sub> (P <sub>II</sub> )	−5.2	−8.7	−10.8	−12.7	−13.1
Δ <i>G</i> <sub>sol</sub> (C <sub>5</sub> )	−5.2	−8.9	−11.2	−13.3	−13.7
Δ <i>G</i> <sub>sol</sub> (α <sub>R</sub> )	−5.7	−9.2	−12.6	−15.0	−15.5
Δ <i>G</i> <sub>ε</sub> (P <sub>II</sub> ) <sup>b</sup>	2.3	2.3	2.3	2.2	2.2
Δ <i>G</i> <sub>ε</sub> (C <sub>5</sub> ) <sup>b</sup>	3.7	3.5	3.3	3.0	3.0
Δ <i>G</i> <sub>ε</sub> (α <sub>R</sub> ) <sup>b</sup>	4.8	4.8	3.5	2.9	2.8

<sup>a</sup> Free energies of solvation (in kcal/mol) in the different solvents are also displayed. Differences are relative to the C<sub>7eq</sub> and C<sub>7ax</sub> conformations for 2 and 3, respectively. Free energies of solvation (Δ*G*<sub>sol</sub>) were computed using the PCM model at the HF/6-311G(d,p) level and considering the molecular geometries optimized in the gas phase at the MP2/6-31G(d) level. <sup>b</sup> Free energy difference at 298 K in solution: Δ*G*<sub>ε</sub> = Δ*G*<sub>gp</sub> + ΔΔ*G*<sub>sol</sub>. The best estimate of Δ*G*<sub>gp</sub> was considered (see Table 8).

Tables 8 and 9 list the free energy differences between the C<sub>7eq</sub> and C<sub>7ax</sub> conformations in the gas phase and in solution, respectively. As can be seen, the entropic contribution destabilizes the latter conformation in the gas phase by about 1 kcal/mol. The best estimate to Δ*G*<sub>gp</sub>, which was obtained at the MP2/



6-31G(d)//B3LYP/6-31G(d) level, is 1.1 kcal/mol. Furthermore, the stability of the  $C_{7eq}$  conformation with respect to the  $C_{7ax}$  structure also increases with the polarity of the environment. Thus,  $\Delta G_\epsilon$  varies from 1.6 kcal/mol for  $\epsilon = 2$  to 2.6 kcal/mol for  $\epsilon = 78.5$ .

Inspection to the  $\Delta G_{sol}$  values indicates that the interaction with the solvent is slightly more favorable for **2** (Table 9) than for **1** (Table 4). However, the most remarkable trend in solution is related to the solvent-induced polarization effects, which are larger for the former compound. Figure 3b shows the variation of the dipole moments with the dielectric constant of the environment for the  $C_{7eq}$  and  $C_{7ax}$  conformations of **2**. As was also found for **1**, the solvent-induced polarization effects sharply increase with the dielectric constant when  $\epsilon \leq 8$ , whereas a flatter variation is obtained for  $\epsilon > 8$ . However, the induced dipole moment is considerably larger for **2** than for **1**. Thus, an organic solvent with  $\epsilon = 2$  induces a change in the dipole moment of 16%, whereas an increase of 27% and 34% is predicted for solvents with  $\epsilon = 4$  and 8, respectively. As expected, the changes induced by polar solvents with  $\epsilon = 33$  and 78.5 (41% and 42%, respectively) are the largest ones. The large solvent-induced changes detected for **2** must be attributed to the presence of the polarizable phenyl side chain.

**Ac-(2*S*,3*R*)c<sub>3</sub>Phe-NHMe (3).** It should be noted that the stereochemical difference between dipeptides **2** and **3** involves the orientation of the phenyl ring with respect to the amide groups (Figure 1). Thus, in **3**, the phenyl ring is fixed in a *cis* relative disposition with reference to the carbonyl substituent ( $\chi_1 \approx 135^\circ$ ), whereas in **2**, the aromatic side chain eclipses the acetylamino moiety. Accordingly, notable conformational differences are expected between the two stereoisomers.

The number of starting points considered for geometry optimizations at the HF/6-31G(d) level was the same as for **2**. Four structures were characterized as minimum energy conformations, which were reoptimized at the B3LYP/6-31G(d) level. Table 5 lists the dihedral angles of the resulting minima, whereas the  $\Delta H_{gp}$  values are compared in Table 6. The lowest energy conformation corresponds to the  $C_{7ax}$ , whereas the  $C_{7eq}$  is not an energy minimum. The latter conformation is strongly disfavored by a repulsive interaction between the carbonyl oxygen of the (2*S*,3*R*)c<sub>3</sub>Phe residue and the  $\pi$  cloud of the phenyl ring. The  $C_{7ax}$  minimum is solely stabilized by an intramolecular hydrogen bond between the two amide groups, with its geometric parameters being  $d(H\cdots O) = 2.007 \text{ \AA}$  and  $\angle N-H\cdots O = 149.3^\circ$  (Figure 5a). Thus, no interaction between the side phenyl ring and the amide groups is established in this case. The opposite situation appears in the  $P_{II}$  conformation, which is stabilized by an  $N-H\cdots\pi$  interaction (Figure 5b). The geometric parameters for such an interaction,  $d_{H\cdots Ph} = 3.034 \text{ \AA}$  and  $\theta = 46.8^\circ$ , are consistent with a tilted arrangement. The  $C_5$  conformation is disfavored by 3.1 kcal/mol with respect to the global minimum at the MP2/6-31G(d)//B3LYP/6-31G(d) level. The intramolecular hydrogen bonding parameters for this conformation, which is displayed in Figure 5c,  $d(H\cdots O) = 2.003 \text{ \AA}$  and  $\angle N-H\cdots O = 113.4^\circ$ , are similar to those obtained for dipeptide **1** (Figure 2b). Furthermore, the side chain disposition allows the existence of an  $N-H\cdots\pi$  interaction for this conformation. The geometric parameters associated with this interaction,  $d_{H\cdots Ph} = 3.134 \text{ \AA}$  and  $\theta = 52.7^\circ$ , support again a tilted structure. The last minimum corresponds to an  $\alpha_R$  conformation (Figure 5d), which is 5.4 kcal/mol less stable than the global minimum. No stabilizing intramolecular interaction either of the  $N-H\cdots\pi$  or of the hydrogen bond type was found for this structure. However, the characterization of a helical

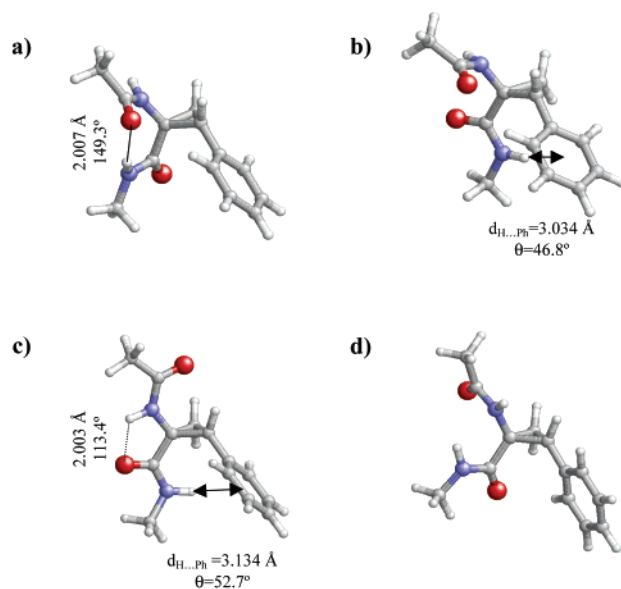


**Figure 5.**  $C_{7ax}$  (a),  $P_{II}$  (b),  $C_5$  (c), and  $\alpha_R$  (d) minimum energy conformations of Ac-(2*S*,3*R*)c<sub>3</sub>Phe-NHMe (**3**) obtained at the B3LYP/6-31G(d) level of theory. Hydrogen bonding distances (H...O) and angles (N-H...O), as well as the parameters associated to the interactions between the N-H bond and the phenyl ring (H...Ph center distance,  $d_{H\cdots Ph}$ ; N-H...Ph plane angle,  $\theta$ ) are indicated.

minimum indicates that this conformation cannot be discarded for larger (2*S*,3*R*)c<sub>3</sub>Phe-containing peptides, where the helix could be stabilized by hydrogen bonds between different residues.

Inspection to the geometric parameters of the cyclopropane ring (Table 7) does not reveal significant differences with respect to those provided for **2**. The  $\angle N-C^\alpha-C'$  angle shows an important conformational dependence. Thus, the  $C_{7ax}$  and  $\alpha_R$  conformations present values close to  $117^\circ$ , whereas tetrahedral ones are adopted by the  $P_{II}$  and  $C_5$  conformations. These trends are in good agreement with the results showed in the previous sections for **1** and **2**.

Inspection to the  $\Delta G_{gp}$  values (Table 8) indicates that the entropic contribution increases the energy gap between the  $C_{7ax}$  and  $P_{II}$  conformations at both the HF/6-31G(d) and B3LYP/6-31G(d) levels of theory. Furthermore, the  $C_5$  conformation is entropically disfavored with respect to the global minimum by 0.7 kcal/mol at the latter level. On the other hand, results displayed in Table 9 show that the solvent tends to stabilize the  $C_5$  and  $\alpha_R$  conformations with respect to the global minimum, an effect that is particularly remarkable in the latter one. Thus, the  $\alpha_R$  structure presents a very favorable electrostatic interaction with the solvent because its dipole moment (5.90 D) is larger than those predicted for the other conformations (Figure 3c). However, the  $C_{7ax}$  structure remains the most favored conformation independently of the dielectric constant of the environment.

Figure 3c shows the variation of the dipole moment with the dielectric constant of the environment for the four minimum energy conformations of **3**. As it can be seen, the solvent-induced polarization effects for this compound depend on the conformation. Thus, the induced dipole moment is very small for the  $C_{7ax}$  conformation (4% and 13% for  $\epsilon = 2$  and 78.5, respectively) but very large for the  $P_{II}$  structure (25% and 62% for  $\epsilon = 2$  and 78.5, respectively). It should be noted that in the former conformation such effects vanish because the polarizable groups are partially buried. Regarding the  $C_5$  and  $\alpha_R$  conformations, a nonpolar solvent with  $\epsilon = 2$  induces a change in the

**TABLE 10: Enthalpy Difference<sup>a</sup> (in kcal/mol) between Ac-(2*S*,3*S*)c<sub>3</sub>Phe-NHMe (2) and Ac-(2*S*,3*R*)c<sub>3</sub>Phe-NHMe (3) and Interaction Energy<sup>b</sup> (in kcal/mol) between the Backbone and the Phenyl Side Chain for Some Selected Minimum Energy Conformations of 2 and 3**

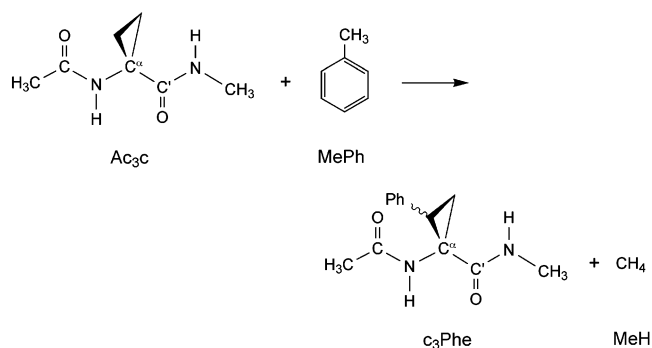
level <sup>c</sup>	$\Delta H^{2-3}$	$\Delta E^{\text{BB/Ph}}$	
		C <sub>7eq</sub> (2)	C <sub>7ax</sub> (3)
MP2/6-31G(d)//HF/6-31G(d)	-0.4	-8.4	-8.0
MP2/6-31G(d)//B3LYP/6-31G(d)	-0.2	-8.6	-8.2

<sup>a</sup>  $\Delta H^{2-3}$  was evaluated considering the global minimum of each dipeptide. <sup>b</sup>  $\Delta E^{\text{BB/Ph}}$  was computed using eq 1 (see text). <sup>c</sup> Level of energy calculation // level of geometry optimization.

dipole moment of 20% and 14%, respectively, whereas a polar solvent like water provides an increase of 54% and 42%, respectively. Again, the large solvent-induced changes detected for the P<sub>II</sub>, C<sub>5</sub>, and  $\alpha_R$  conformations should be attributed to the presence of the polarizable phenyl side chain.

**Backbone...Side Chain Interactions in c<sub>3</sub>Phe.** The results displayed in previous sections suggest that the backbone...phenyl side chain interactions could be responsible for the conformational differences between dipeptides 2 and 3. It is hoped to gain some insights about such interactions by comparing their energies, which could be directly subtracted because they only differ from each other in the stereochemistry of the substituted  $\beta$  carbon. Table 10 shows the enthalpy difference between 2 and 3,  $\Delta H^{2-3}$ , evaluated by considering their global minima, i.e., C<sub>7eq</sub> and C<sub>7ax</sub> for 2 and 3, respectively. It should be noted that  $\Delta H^{2-3}$  provides an estimation of the relative stability between such two stereoisomers. Only values derived from MP2 energies have been included in Table 10 because this method is more appropriate to consider electron correlation effects than the HF and B3LYP ones. However, it should be noted that dipeptide 2 is more stable at all of the levels of theory.

A quantitative analysis of the backbone...phenyl interaction has been used to rationalize this feature. For this purpose, the isodesmic reaction displayed in the following scheme has been considered.<sup>28</sup>

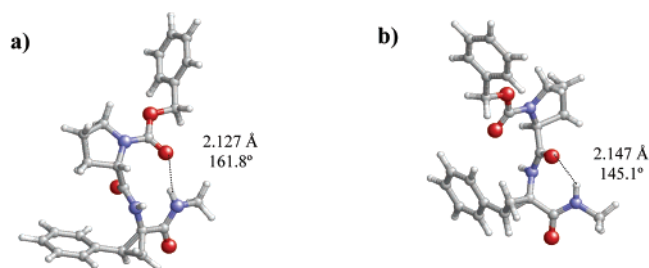


For each compound, the interaction energy between the backbone and the phenyl side chain,  $E^{\text{BB/Ph}}$ , in the global minimum was estimated according to eq 1:

$$E^{\text{BB/Ph}} = E^{\text{c3Phe}} - [(E^{\text{Ac3c}} - E^{\text{MeH}}) + E^{\text{MePh}}] \quad (1)$$

where  $E^{\text{c3Phe}}$  corresponds to the electronic energy of the global minimum for 2 or 3 and  $E^{\text{Ac3c}}$  is the electronic energy for the C<sub>7</sub> conformation of 1. Results are displayed in Table 10.

As can be seen, the values of  $E^{\text{BB/Ph}}$  reveal a strong backbone...side chain attractive interaction for the two compounds. Thus, the phenyl ring is a bulky group with a large amount of electron density, able to interact with the dipeptide backbone in both cases. However, the  $E^{\text{BB/Ph}}$  contribution is only

**Figure 6.**  $\beta$ -Turn (a) and C<sub>7</sub> (b) minimum energy conformations of Z-L-Pro-(2*S*,3*S*)c<sub>3</sub>Phe-NHMe obtained in the HF/6-31G(d) level of theory. Hydrogen bonding distances (H...O) and angles (N-H...O) are indicated.**TABLE 11: Dihedral Angles (in Degrees) and Energy Differences in the Gas Phase (in kcal/mol) for the Minimum Energy Conformations of the Model Tripeptide Z-L-Pro-(2*S*,3*S*)c<sub>3</sub>Phe-NHMe Obtained at the HF/6-31G(d) Level**

fragment	torsional angle	X-ray <sup>a</sup>	$\beta$ -turn	C <sub>7</sub>
Z <sup>b</sup> Pro	$\omega$	178.2	176.4	175.3
	$\varphi$	-51.0	-53.7	-55.2
(2 <i>S</i> ,3 <i>S</i> )c <sub>3</sub> Phe	$\psi$	134.2	133.7	141.3
	$\omega$	173.8	179.0	-169.6
	$\varphi$	72.3	70.0	-82.2
	$\psi$	-0.2	9.1	30.2
	$\omega$	-173.8	-174.8	-177.8
	$\chi_1$	7.6	7.5	7.4
	$\chi_2$	-47.1	-97.7	-66.5
	$\Delta E$	-	0.0 <sup>c</sup>	1.9

<sup>a</sup> From ref 13a. <sup>b</sup> Benzyloxycarbonyl group. <sup>c</sup>  $E = -1387.417039$  au.

slightly more favorable for the global minimum of 2 than for that of 3. As can be seen in Figures 4a and 5a, the most notable difference between such two conformations is the presence of an N-H... $\pi$  interaction in the former case. Accordingly, the difference  $\Delta^{2,3} = [E^{\text{BB/Ph}}(\text{C}_{7\text{eq}}, 2) - E^{\text{BB/Ph}}(\text{C}_{7\text{ax}}, 3)]$  should provide a reasonable estimation of the N-H... $\pi$  interaction because the other interactions are expected to be similar for the two compounds. Energy calculations lead to a  $\Delta^{2,3}$  value of -0.4 kcal/mol, a result that is consistent with the values obtained for  $\Delta H^{2-3}$ .

**Calculations on Z-L-Pro-(2*S*,3*S*)c<sub>3</sub>Phe-NHMe.** The crystal molecular structure of Z-L-Pro-(2*S*,3*S*)c<sub>3</sub>Phe-NHMe was reported in a recent work.<sup>13a</sup> The molecule adopts a type II  $\beta$ -turn stabilized by a hydrogen bond between the terminal benzyloxycarbonyl and methylamide groups that closes a ten-membered ring. The (2*S*,3*S*)c<sub>3</sub>Phe residue occupies the *i*+2 position and exhibits  $\varphi$ ,  $\psi$  dihedral angles near 70°, 0°. As discussed above, this conformation was not detected as a minimum in the potential energy surface of dipeptide 2. However, it would be interesting to know if the  $\beta$ -turn is a minimum accessible to (2*S*,3*S*)c<sub>3</sub>Phe when incorporated into longer peptide chains.

With this aim, the molecular conformation found in the solid state for Z-L-Pro-(2*S*,3*S*)c<sub>3</sub>Phe-NHMe was fully optimized at the HF/6-31G(d) level. The resulting minimum (a) is displayed in Figure 6a, whereas Table 11 compares the dihedral angles with those determined by X-ray crystallography. As can be seen, the optimized structure is able to retain the initial  $\beta$ -turn conformation, with the backbone dihedral angles being very similar to those observed in the crystal. The largest change occurs for the dihedral of the phenyl side chain  $\chi_2$ , which evolves from a gauche<sup>-</sup> conformation to a skew<sup>-</sup> disposition, probably because of the absence of packing effects.



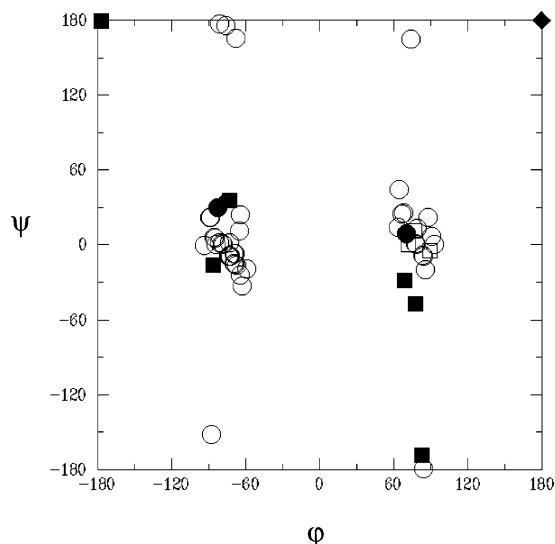


**Figure 7.** Comparison between the conformational preferences observed (CSDB) and predicted (this work) for diamide derivatives of 1-aminocyclopropanecarboxylic acids. Empty circles (○) correspond to all of the observed conformations for cyclopropaneamino acids (44 conformations) with exception of  $c_3$ Phe (3 conformations), which are indicated by empty squares (□). Filled symbols correspond to the minimum energy conformations predicted for Ac-Ac $_3$ c-NHMe (◆), Ac-(2*S*,3*S*) $c_3$ Phe-NHMe and Ac-(2*S*,3*R*) $c_3$ Phe-NHMe (■), and Z-L-Pro-(2*S*,3*S*) $c_3$ Phe-NHMe (●).

We have also investigated the stability of the  $C_{7eq}$  conformation, which was identified as the global minimum for **2**, in the Z-L-Pro-(2*S*,3*S*) $c_3$ Phe-NHMe peptide. For this purpose, the experimentally observed conformation was changed by replacing the dihedral angles of the (2*S*,3*S*) $c_3$ Phe residue by those obtained for the  $C_{7eq}$  conformation of dipeptide **2**. Complete geometry optimization at the HF/6-31G(d) level led to the structure shown in Figure 6b (b), which is characterized by a  $\gamma$ -turn ( $C_7$ ) centered at the  $c_3$ Phe residue, and the conformational parameters are listed in Table 11. Moreover, the resulting dihedral angles for (2*S*,3*S*) $c_3$ Phe deviate by less than  $2^\circ$  with respect to those of the  $C_{7eq}$  minimum characterized for **2**. However, the conformation of the Pro residue changes from the twisted  $C^\beta$ -endo/ $C^\gamma$ -exo to the envelope  $C^\gamma$ -exo. The relative energies (Table 11) indicate that conformation b is 1.9 kcal/mol less stable than a. However, this energy difference can be notably influenced by the presence of the Pro residue, which tends to be involved in the position  $i+1$  of  $\beta$ -turns<sup>29</sup> and, therefore, cannot be solely ascribed to the differential preferences of (2*S*,3*S*) $c_3$ Phe for the  $\beta$ - and  $\gamma$ -turn dispositions.

**Survey of the Conformational Preferences of Cyclopropaneamino Acids.** The structure of diamide derivatives of 1-aminocyclopropanecarboxylic acids was obtained from the Cambridge Structural Data Base (CSDB).<sup>30</sup> Figure 7 represents the conformational angles  $\varphi$  and  $\psi$  of the structures determined by X-ray crystallography together with all of the theoretical minima characterized for **1–3** and the two structures computed for Z-L-Pro-(2*S*,3*S*) $c_3$ Phe-NHMe. As can be seen, there is a good agreement between the experimental and theoretical conformations. Thus, there is a correspondence between the theoretical minima found for **1** and **2**, with exception of the  $C_5$  structure predicted for **1**, and the regions of the  $\varphi,\psi$  map associated to the observed conformations. As for **3**, no comparison can be established because of the absence of crystallographic data for (2*S*,3*R*) $c_3$ Phe-containing peptides. It should be emphasized that the cyclopropaneamino acids used to generate the  $\varphi,\psi$  map bear a wide variety of chemical groups as side chains. This feature

indicates that the conformational preferences of the Ac $_3$ c derivatives are strongly influenced by the cyclopropane ring, even though they are modulated by the interactions between the side chain and the backbone.

## Summary

We have theoretically examined the influence of the phenyl side chain on the conformational features of cyclopropaneamino acid derivatives using the dipeptide models **1–3**. The results can be summarized as follows:

(1) Calculations on **1** show that the B3LYP/6-31G(d) method is more suitable than the HF/6-31G(d) one to explore the conformational preferences of small model peptides. Furthermore, the description of this compound is not substantially improved by using more sophisticated theoretical levels than the B3LYP/6-31G(d). Dipeptide **1** only presents two different minimum energy conformations: the  $C_7$ , which is the global minimum, and the  $C_5$  structures. The free energy difference between the two conformations in the gas phase is 4.5 kcal/mol and increases with the polarity of the environment.

(2) Two minimum energy conformations were characterized for **2**, the  $C_{7eq}$  resulting 1.1 kcal/mol more stable in the gas phase than the  $C_{7ax}$ . The main difference between such two minima is the presence of an attractive N–H... $\pi$  interaction in the global minimum. On the other hand, four minimum energy conformations were predicted for **3**:  $C_{7ax}$ ,  $P_{II}$ ,  $C_5$ , and  $\alpha_R$ . The former is the most stable conformation, with the remaining structures being less stable by 2.4, 3.8, and 5.4 kcal/mol, respectively, in the gas phase. Furthermore, the  $P_{II}$  and  $C_5$  conformations present a stabilizing N–H... $\pi$  interaction. The free energy differences increase with the polarity of the environment for **2**, whereas they decrease for **3**.

(3) The phenyl side group increases the magnitude of the solvent-induced polarization effects. Thus, in general, such effects are larger for the  $c_3$ Phe dipeptides than for the Ac $_3$ c derivative. In addition, the stereochemistry of the phenyl ring controls some structural properties of the  $c_3$ Phe residue. Specifically, the geometry of the N–H... $\pi$  interaction seems to be highly dependent on this trend. The amide and the phenyl groups are tilted for the  $C_{7eq}$  conformation of **2**, whereas for the  $C_5$  and  $P_{II}$  minima of **3**, such groups adopt a perpendicular arrangement. Furthermore, the strength of the backbone...phenyl interactions also depends on the position of the ring.

(4) Hyperconjugative effects between the cyclopropane ring and the adjacent C=O moiety were detected for all of the compounds investigated in this work. Accordingly, computational studies based on classical potential functions require a suitable force-field parametrization in order to take into account such an electronic effect.

**Acknowledgment.** The authors are indebted to the “Centre de Supercomputació de Catalunya” (CESCA) for computational facilities. Financial support from the “Ministerio de Ciencia y Tecnología” (Project PPQ2001-1834 and “Ramón y Cajal” contract for A. I. J.) is gratefully acknowledged.

**Supporting Information Available:** The B3LYP and MP2 geometrical parameters. This material is available free of charge via the Internet at <http://pubs.acs.org>.

## References and Notes

- (1) (a) Balaram, P. *Curr. Opin. Struct. Biol.* **1992**, 2, 845. (b) Di Blasio, B.; Pavone, V.; Lombardi, A.; Pedone, C.; Benedetti, E. *Biopolymers* **1993**, 33, 1037. (c) Gante, J. *Angew. Chem., Int. Ed. Engl.* **1994**, 33, 1699. (d)

- Marraud, M.; Aubry, A. *Biopolymers* **1996**, *40*, 45. (e) Benedetti, E. *Biopolymers* **1996**, *40*, 3.
- (2) (a) Karle I. L.; Balam, P. *Biochemistry* **1990**, *29*, 6747. (b) Karle, I. L.; Flippen-Anderson, J. L.; Uma, K.; Balam, P. *Proteins* **1990**, *7*, 62. (c) Pavone, V.; Benedetti, E.; Di Blasio, B.; Pedone, C.; Santini, A.; Bavoso, A.; Toniolo, C.; Crisma, M.; Sartore, L. *J. Biomol. Struct. Dyn.* **1990**, *7*, 1321.
- (3) (a) Alemán, C. *Biopolymers* **1994**, *34*, 841. (b) Huston, S. E.; Marshall, G. R. *Biopolymers* **1994**, *34*, 75. (c) Zhang, L.; Herman, J. J. *Am. Chem. Soc.* **1994**, *116*, 11915. (d) Alemán, C.; Roca, R.; Luque, F. J.; Orozco, M. *Proteins* **1997**, *28*, 83. (e) Improt, R.; Nega, N.; Alemán, C.; Barone, V. *Macromolecules* **2001**, *34*, 7550.
- (4) (a) Alemán, C. *J. Phys. Chem. B* **1997**, *101*, 5046. (b) Gould, I. R.; Kollman, P. A. *J. Phys. Chem.* **1992**, *96*, 9255.
- (5) Hruby, V. J.; Li, G.; Haskell-Luevano, C.; Shenderovich, M. *Biopolymers* **1997**, *43*, 219.
- (6) (a) Mitchell, J. B. O.; Nandi, C. L.; McDonald, I. K.; Thornton, J. M. *J. Mol. Biol.* **1994**, *239*, 315. (b) Mitchell, J. B. O.; Nandi, C. L.; Ali, S.; McDonald, I. K.; Thornton, J. M. *Nature* **1993**, *366*, 413.
- (7) Worth, G. A.; Wade, R. C. *J. Phys. Chem.* **1995**, *99*, 17473.
- (8) Mapelli, C.; Stammer, C. H.; Lok, S.; Mierke, D. F.; Goodman, M. *Int. J. Pept. Protein Res.* **1988**, *32*, 484.
- (9) (a) Mapelli, C.; Kimura, H.; Stammer, C. H. *Int. J. Pept. Protein Res.* **1986**, *28*, 347. (b) Shimohigashi, Y.; Takano, Y.; Kamiya, H.; Costa, T.; Herz, A.; Stammer, C. H. *FEBS Lett.* **1988**, *233*, 289. (c) Kimura, H.; Stammer, C. H.; Shimohigashi, Y.; Ren-Lin, C.; Stewart, J. *Biochem. Biophys. Res. Commun.* **1983**, *115*, 112.
- (10) Déry, O.; Josien, H.; Grassi, J.; Chassaing, G.; Couraud, J. Y.; Lavielle, S. *Biopolymers* **1996**, *39*, 67.
- (11) (a) Burgess, K.; Ho, K.-K.; Pal, B. *J. Am. Chem. Soc.* **1995**, *117*, 3808. (b) Malin, D. H.; Lake, J. R.; McDermitt, L. S.; Smith, D. A.; Witherspoon, W. E.; Jones, J. A.; Schumann, M. D.; Payza, K.; Ho, K.-K.; Burgess, K. *Peptides* **1996**, *17*, 83.
- (12) Ogawa, T.; Yoshitomi, H.; Kodama, H.; Waki, M.; Stammer, C. H.; Shimohigashi, Y. *FEBS Lett.* **1989**, *250*, 227.
- (13) (a) Jiménez, A. I.; Cativiela, C.; Aubry, A.; Marraud, M. *J. Am. Chem. Soc.* **1998**, *120*, 9452. (b) Jiménez, A. I.; Vanderesse, R.; Marraud, M.; Aubry, A.; Cativiela, C. *Tetrahedron Lett.* **1997**, *38*, 7559.
- (14) Moye-Sherman, D.; Jin, S.; Li, S.; Welch, M. B.; Reibenspies, J.; Burgess, K. *Chem. Eur. J.* **1999**, *5*, 2730.
- (15) Brooks, B.; Brucoleri, R.; Olafson, H.; States, D.; Swaminathan, S.; Karplus, M. *J. Comput. Chem.* **1983**, *4*, 187.
- (16) (a) Barone, V.; Fraternali, F.; Cristinziano, P. L.; Lelj, F.; Rosa, A. *Biopolymers* **1988**, *27*, 1673. (b) Taylor, E. W.; Wilson, S.; Stammer, C. H. In *Sweeteners. Discovery, Molecular Design and Chemoreception*; Walters, D. E., Orthoefer, F. F., DuBois, G. E., Eds.; ACS Symposium Series 450; American Chemical Society: Washington, DC, 1991; pp 162–175. (c) Alemán, C.; Casanovas, J.; Galembeck, S. E. *J. Comput. Aided Mol. Design* **1998**, *12*, 259. (d) Gómez-Catalán, J.; Alemán, C.; Pérez, J. J. *Theor. Chem. Acc.* **2000**, *103*, 380.
- (17) (a) Cramer, C. J. *J. Mol. Struct. (THEOCHEM)* **1996**, *370*, 135. (b) Volltrauer, H. N.; Schwendeman, H. J. *Chem. Phys.* **1971**, *54*, 260.
- (18) (a) Frisch, M. J.; Trucks, G. W.; Schlegel, H. B.; Scuseria, G. E.; Robb, M. A.; Cheeseman, J. R.; Zakrzewski, V. G.; Montgomery, J. A., Jr.; Stratmann, R. E.; Burant, J. C.; Dapprich, S.; Millam, J. M.; Daniels, A. D.; Kudin, K. N.; Strain, M. C.; Farkas, O.; Tomasi, J.; Barone, V.; Cossi, M.; Cammi, R.; Mennucci, B.; Pomelli, C.; Adamo, C.; Clifford, S.; Ochterski, J.; Petersson, G. A.; Ayala, P. Y.; Cui, Q.; Morokuma, K.; Malick, D. K.; Rabuck, A. D.; Raghavachari, K.; Foresman, J. B.; Cioslowski, J.; Ortiz, J. V.; Stefanov, B. B.; Liu, G.; Liashenko, A.; Piskorz, P.; Komaromi, I.; Gomperts, R.; Martin, R. L.; Fox, D. J.; Keith, T.; Al-Laham, M. A.; Peng, C. Y.; Nanayakkara, A.; Gonzalez, C.; Challacombe, M.; Gill, P. M. W.; Johnson, B. G.; Chen, W.; Wong, M. W.; Andres, J. L.; Head-Gordon, M.; Replogle, E. S.; Pople, J. A. *Gaussian 98*, revision A.7; Gaussian, Inc.: Pittsburgh, PA, 1998. (b) Frisch, M. J.; Trucks, G. W.; Schlegel, H. B.; Gill, P. M. W.; Johnson, B. G.; Robb, M. A.; Cheeseman, J. R.; Keith, T.; Petersson, G. A.; Montgomery, J. A.; Raghavachari, K.; Al-Laham, M. A.; Zakrzewski, V. G.; Ortiz, J. V.; Foresman, J. B.; Cioslowski, J.; Stefanov, B. B.; Nanayakkara, A.; Challacombe, M.; Peng, C. Y.; Ayala, P. Y.; Chen, W.; Wong, M. W.; Andres, J. L.; Replogle, E. S.; Gomperts, R.; Martin, R. L.; Fox, D. J.; Binkley, J. S.; Defrees, D. J.; Baker, J.; Stewart, J. P.; Head-Gordon, M.; Gonzalez, C.; Pople, J. A. *Gaussian 94*, revision B.3; Gaussian, Inc.: Pittsburgh, PA, 1995.
- (19) Hariharan, P. C.; Pople, J. A. *Chem. Phys. Lett.* **1972**, *16*, 217.
- (20) Lee, C.; Yang, W.; Parr, R. G. *Phys. Rev. B* **1993**, *37*, 785.
- (21) Møller, C.; Plesset, M. S. *Phys. Rev.* **1934**, *46*, 618.
- (22) (a) Miertus, S.; Scrocco, E.; Tomasi, J. *Chem. Phys.* **1981**, *55*, 117. (b) Tomasi, J.; Persico, M. *Chem. Rev.* **1994**, *94*, 2027.
- (23) (a) Orozco, M.; Luque, F. J. *J. Am. Chem. Soc.* **1995**, *117*, 1378. (b) Alemán, C.; Navarro, E.; Puiggalí, J. *J. Org. Chem.* **1995**, *60*, 6135. (c) Colominas, C.; Orozco, M.; Luque, F. J.; Borrell, J. I.; Teixidó, J. *J. Org. Chem.* **1998**, *63*, 4947.
- (24) (a) Böhm, H.-J.; Brode, S. *J. Am. Chem. Soc.* **1991**, *113*, 7129. (b) Alemán, C.; Puiggalí, J. *J. Phys. Chem. B* **1997**, *101*, 3441. (c) Alemán, C. *J. Phys. Chem. A* **2000**, *104*, 7612.
- (25) (a) Valle, G.; Crisma, M.; Toniolo, C.; Holt, E. M.; Tamura, M.; Bland, J.; Stammer, C. H. *Int. J. Pept. Protein Res.* **1989**, *34*, 56. (b) Benedetti, E.; Di Blasio, B.; Pavone, V.; Pedone, C.; Santini, A.; Crisma, M.; Valle, G.; Toniolo, C. *Biopolymers* **1989**, *28*, 175. (c) Benedetti, E.; Di Blasio, B.; Pavone, V.; Pedone, C.; Santini, A.; Barone, V.; Fraternali, F.; Lelj, F.; Bavoso, A.; Crisma, M.; Toniolo, C. *Int. J. Biol. Macromol.* **1989**, *11*, 353. (d) Fabiano, N.; Valle, G.; Crisma, M.; Toniolo, C.; Saviano, M.; Lombardi, A.; Isernia, C.; Pavone, V.; Di Blasio, B.; Pedone, C.; Benedetti, E. *Int. J. Pept. Protein Res.* **1993**, *42*, 459.
- (26) Alemán, C.; Casanovas, J. *Biopolymers* **1995**, *36*, 71.
- (27) Jiménez, A. I.; Cativiela, C.; Gómez-Catalán, J.; Pérez, J. J.; Aubry, A.; París, M.; Marraud, M. *J. Am. Chem. Soc.* **2000**, *122*, 5811.
- (28) Viviani, W.; Rivail, J.-L.; Perczel, A.; Csizmadia, I. G. *J. Am. Chem. Soc.* **1993**, *115*, 8321.
- (29) MacArthur, M. W.; Thornton, J. M. *J. Mol. Biol.* **1991**, *218*, 397.
- (30) Allen, F. H.; Davies, J. E.; Galloy, J. J.; Johnson, O.; Kennard, O.; Macrae, C. F.; Mitchell, E. M.; Mitchell, G. F.; Smith, J. M.; Watson, D. G. *J. Chem. Inf. Comput. Sci.* **1991**, *31*, 187.